Qualification of Hairpin Motors Insulation for Automotive Applications

Qualification of Hairpin Motors Insulation for Automotive Applications

Paolo Mancinelli, Simone Stagnitta, and Andrea Cavallini

***Abstract*—This paper is focused on the reliability evaluation of an electric vehicle (EV) motor based on hairpin technology. Besides bearings (not discussed here), the weak point of an electric motor is its insulating system. For inverter-fed motors, the inception of partial discharges might lead to failure in a matter of days, and thus, deserves particular attention. Qualification and lifetime evaluation of inverter-fed machines are described in IEC 60034-18-41, which specifies accelerated aging procedures and considers partial discharge inception as the end-of-life criterion. This standard was used as a reference for this paper. The only exception is that insulation models were subjected to the mechanical stress profile reported in the ISO 16750-3-2012 standard since an automotive motor is subject to significant vibrations during its operation. From the tests performed, we observed that, with the hairpin technology, turn-to-turn is the weakest link in the insulation system. All the insulation models were partial discharge (PD) free from the beginning of the tests to breakdown and the root cause for breakdown was, in all cases, traced back to cracks on the surface of the insulation. This suggests that, depending on insulating enamel thickness and conductor geometry, some insulation systems are intrinsically PD free by design, despite the effect of aging. Considering the severe vibration profiles typical of EVs, and the principal breakdown mechanism (cracking of the insulation), mechanical stress coupled with thermal stress appears as the main aging driver. Therefore, this paper spotlights the lack of proper standards for the qualification of automotive electric motors and hints at the possibility that IEC 60034-18-41 considers dealing with motors that might be intrinsically partial discharge free even after long-term exposure to operational stresses.**

***Index Terms*—Aging, automotive, electrical motor qualification, lifetime analysis, partial discharge (PD).**

I. Introduction

IN THE last two decades, environmental protection agencies pushed the automotive industry toward more stringent emission limits for internal combustion engines (ICEs), up to a point where a further reduction of actual emissions levels is not easily achievable. As a result, the manufacturer's declared consumption and emission data are sometimes not clearly replicable, as recent events showed [1].

This has led to investigating new solutions for the sustainability of urban mobility. Hybrid and electric vehicles (HVs and EVs) are the solutions commercially available to date. While HVs had a sufficient market penetration in the last years, EVs need further development to be competitive yet. The weak points of this technology are the limited operating range and the long time required to the storage systems to be charged.

Actually, for urban mobility, where the distance traveled on a daily basis is limited, the EVs may become competitive or even preferable than ICEs, due to the better performance at the lower speed in terms of both acceleration and efficiency. Moreover, the mechanical complexity of an electrical motor is lower than an ICE, with consequently lower maintenance costs [2].

The main limit to EVs penetration in the urban mobility market is their actual high cost. This is due to the storage systems but also to the electrical motors, whose production costs are still high (mostly due to the high cost of permanent magnets). For this reason, several research projects are underway to bridge the gap between EVs and ICEs. One of such projects is the EU-funded SyrNemo project, whose target is the development of an innovative synchronous reluctance machine with higher power density and higher driving cycle efficiency at lower cost than the state of the art permanent magnet (PM) synchronous machines [3]–[6].

Bar windings are used in order to simplify the manufacturing, to give to the stator a good robustness and to increase the slot fill factor, and consequently, the power density. The target lifetime of the insulation is 10 000 h.

The life of an electrical motor is mostly limited by the reliability of the insulating system [7]. For EVs, the electrical stress associated with the use of power electronics and the significant levels of mechanical stress due to the vehicle movement, call for a thorough demonstration of the capability of the insulation to fulfill its duties. Therefore, the aim of this paper is to discuss an appropriate method to validate an electrical motor with hairpin technology windings for automotive applications.

II. Electrical Insulation System Reliability

Electrical insulation systems for low-voltage machines are mostly based on organic material [8]. Thus, they are subjected to aging due to different phenomena (embrittlement, cracking, erosion, pollution absorption, etc.). Higher temperatures and temperature cycles are the most common aging factors for organic materials [9]. Mechanical stress and chemical agents are other common factors [10], [11].

Manuscript received July 13, 2016; revised October 10, 2016; accepted October 10, 2016. Date of publication October 20, 2016; date of current version May 18, 2017. Paper 2016-EMC-0460.R1, approved for publication in the IEEE Transactions on Industry Applications by the Electric Machines Committee of the IEEE Industry Applications Society. This work was supported by the European Union's Seventh Framework Programme FP7/2013-2016 under REA Grant 605075.

The authors are with the Laboratory of Innovation Technologies, Department of Electrical Electronic and Information Engineering, University of Bologna, 40126 Bologna, Italy (e-mail: paolo.mancinelli@unibo.it; simone.stagintta@studio.unibo.it; andrea.cavallini@unibo.it).

Color versions of one or more of the figures in this paper are available online at http://ieeexplore.ieee.org.

Electrical stress is another key factor for the reduction of the lifetime of the insulation itself [12], [13]. However, in a low voltage motor, whenever the voltage is below the partial discharge inception voltage (PDIV), the degradation rate associated with electrical stress can be neglected (partial discharges, PDs, are low energy discharges that do not short circuit the insulation [14]). However, in a poorly designed or manufactured insulation system, PD might be incepted and this will cause a fast, irreversible, damage to the insulating system, leading to breakdown.

The use of power electronics has changed the aforementioned picture. As a matter of fact, inverter surges are prone to give: 1) reflections at the cable/motor interface due to surge impedance mismatch [15], [16], and 2) uneven turn voltage distributions associated with the high slew rates of the surges [17]. Both phenomena contribute to increase the electrical stress that might become large enough to sustain PD activity. If PDs are incepted once, the fast voltage polarity reversals associated with the carrier frequencies of tens of kilohertz can induce extremely large PD repetition rates, compromising the insulation in a matter of days, sometimes hours.

The International Electrotechnical Commission (IEC) has promoted documents to tackle this problem. These documents specify qualification procedures to ensure that the insulation design and manufacturing are good enough to ensure satisfactory reliability under inverter surges of different severity. EV motors make no exception; their safety and criticality issues call for an accurate qualification of the insulation.

Qualification tests for electrical motors having purely organic insulation system (referred to as Type I) are described in the IEC 60034-18-41 standard [18]. A qualification test is an accelerated life test that allows us to predict the lifetime of components subject to determined stress factors. To accelerate the tests, stress levels higher than those experienced in service must be employed, and mathematical methods are used to extrapolate the life of the system at the service stress levels. Differently from conventional motors, where the endpoint of the test is the insulation breakdown [19], for an inverter-fed motor, [18] dictates that the endpoint is the inception of PD. The rationale is that the remaining life after PD inception is negligible in comparison with the time under thermal and mechanical stresses needed to bring the insulation to a point where PD can be incepted.

According to the aforementioned, except for the definition of the endpoint, the qualification procedures described in [18] are similar to those already provided in [19], and are based on aging subcycles where temperature and mechanical stress levels are raised in comparison with those experienced in operation. According to IEC 60505 [20], to deal with stress synergies, the simultaneous applications of different stress as, e.g., thermal and mechanical stress, is preferable to sequential aging subcycles (i.e., subcycles where thermal and mechanical stress are applied sequentially).

For tests at increased temperatures, [19] prescribes the temperatures and lengths of aging subcycle depending on the class temperature of the insulation. Indicatively, the length of the single subcycle should be sufficient to bring an average specimen to breakdown in about ten cycles.

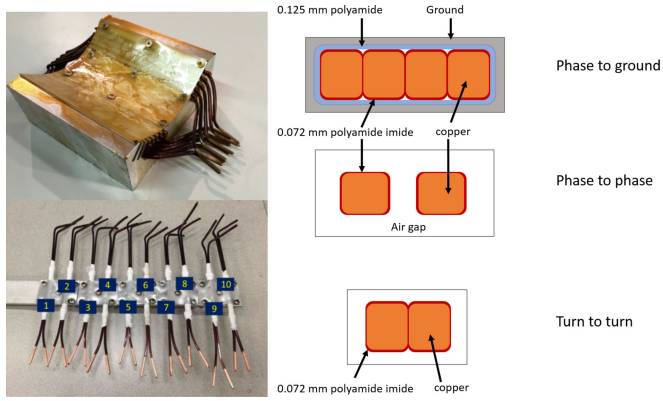

Fig. 1. Structure of the samples used for qualification tests.

The IEC 60034-18-41 standard [18] recommended the test voltage values to be adopted for each sample and for each insulation subsystem to determine whether it is PD free or not. These values are calculated from the inverter dc bus voltage multiplied by a series of different factors to be chosen in regard to the operating condition of the insulation system.

A key issue in the IEC 60034-18-41 standard [18] is the need for a reference insulation system to be compared with the new system under investigation. This reference insulation performance should have been established by satisfactory service experience. For small medium enterprises or when an established, proven insulation system is freshly applied to inverter-fed machines, such a reference system might not be available.

III. Materials and Method

A. Syrnemo Stator and Specimens

The Syrnemo motor stator is designed with 24 slots and each slot lodges four bars of a single phase. Slot liners are used to prevent abrasion of the bar insulation during manufacturing (when bars are inserted in the slot) and during operation (due to electrodynamic forces). Since the motor is fully pitched, phases are separated by air gaps in the end winding, and aramidic paper spacers are not necessary.

The following two different types of samples were employed for the qualification:

1) formettes, to test the phase-to-phase and phase-to-ground insulation;
2) coupled bars, to test the turn-to-turn insulation.

The pictures and sketches in Fig. 1 highlight the structure of the samples. The formettes reproduce a quarter of the Syrnemo motor stator, with the bars held in their slots and covered by the slot liners. The coupled bars are held together with polytetrafluoroethylene (PTFE) tape and connected to an aluminum rod.

The conductors are commercially available copper bars with a double layer coating; the inner one is made by polyesterimide, while the overcoat is made by polyamide-imide. In the formettes, the slot liners, are made by 0.125-mm thick polyimide film (aramidic paper). The formettes were varnished with a commercial polyester resin (Dolphon CC-1105). The coupled

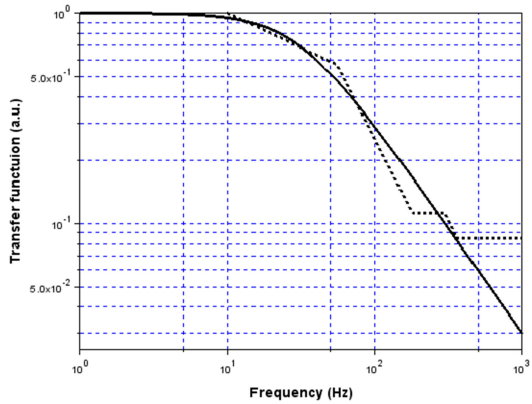

Fig. 2. Dotted line: Spectrum of mechanical vibrations within an EV, after [21]. Continuous line: Frequency response of a low-pass filter with 30-Hz cutoff frequency.

were not varnished, considering this situation as a worst case for PD inception.

B. Qualification and Testing Methodology

As discussed previously, aging of organic materials is an unavoidable phenomenon associated with a number of stress factors. Each of these factors decreases the lifetime and when some of them are occurring simultaneously, it is preferable to apply the stresses simultaneously [20].

For EV motors, the stress factors that pose major concerns are as follows:

1) larger vibrations due to the vehicles movement;
2) larger electrical stress due to
    a) inverter surge reflections;
    b) uneven turn voltage distribution.

Larger electrical stress levels are taken into account in [18] by proper definition of the test voltages used to assess whether PDs are incepted or not within the stator. The standard deals with the cable/motor surge impedance reflections by an overshoot factor (that depends on both the cable length and surge rise time), and provides some worst case factors to tackle 2b. It should be pointed out that, given the limited length of the cables connecting the motor to the inverter, and the hairpin structure of the stator winding, the electrical stress in an EV motor could not be as large as in a, e.g., submerged pump motor (connected to the inverter with long cables) having random wound windings.

The aging process selected in this paper resorts to a multifactorial thermomechanical stress; the vibrations were applied to the insulation models during all the aging process at each temperature. This choice permits taking into account possible synergistic effects of the combination of these two stresses on the lifetime of the insulation. The mechanical stress spectrum on devices inside a vehicle during its movement is described in ISO 16750-3-2012 [21] standard, and is reported in Fig. 2. The vibrations are spread on a wide range of frequencies (the systems behaves similarly to a low-pass filter with 30-Hz cutoff frequency), while the average RMS value of vibrations is 2.84 g_{rms}. A pseudorandom Gaussian signal having the same power density as that reported in Fig. 2 was used to drive the modal shaker. The gain of the shaker was adjusted to achieve the correct g_{rms} value.

TABLE I
TEMPERATURES AND SUBCYCLES LENGTH

Test #	Aging Temperature (°C)	Length of Subcycle (days)
1	250	1–2
2	240	2–3
3	220	7–10

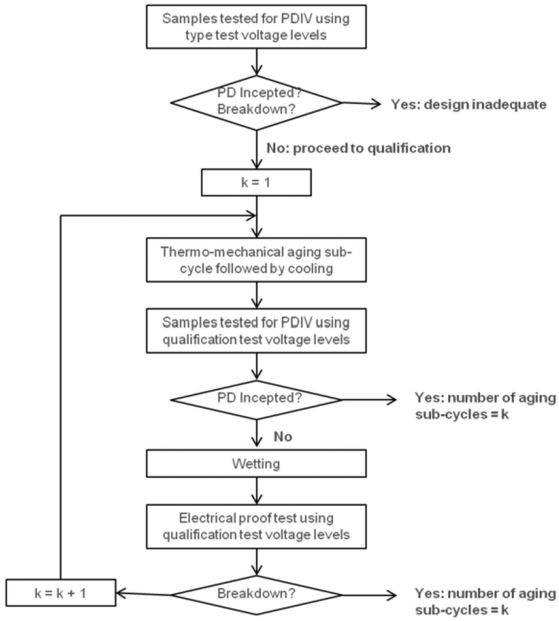

Fig. 3. Test procedure flow chart.

According to [19], the aging temperatures should be chosen following the temperature class of the insulation system. In this paper, considering the hot-spot temperature of the motor, reference was made to a 180 °C class. Therefore, following [19], the maximum aging temperature was 250 °C. The other two values of temperature chosen for the tests, which are required to extrapolate a correct value of lifetime at operating conditions, were 240 °C and 220 °C (see Table I). The subcycle lengths have been chosen according to [19] and shown in Table I. It is worthwhile to observe that the two highest temperatures are separated by 10 °C, contrarily to the prescription of 20 °C reported in [19]. This choice was made to shorten the qualification procedure and meet project deadlines. Clearly it was justified by the fact that the motor target lifetime was 10 000 h, while [19] aims at defining the temperature Index at 20 000 h. Per each temperature level, tests were carried out on one formette (corresponding to five coils in parallel) and on ten coupled bars.

At the end of each aging subcycle, a PDIV test using the qualification voltage is carried out. The samples that passed the test were set in a humidity chamber in saturated air at 25 °C and 100% relative humidity, and then, again electrically proven. In this way, another environmental stress was added to the aging of each subcycle. The test sequence employed is summarized in Fig. 3.

TABLE II
TEST VOLTAGE VALUES FOR THE DIFFERENT SUBSYSTEMS

Insulation subsystem	U_{dc}(V)	OF	U_p(V)	K	EF	U_{test} ($\mathrm{V_{peak}}$)	U_{test} ($\mathrm{V_{rms}}$)
Phase-to-phase	400	1.5	600	1	1.63	978	699
Phase-to-ground	400	1.5	600	0.7	1.38	580	414
Turn-to-turn	400	1.5	600	0.7	1.63	685	489

The presence of PD was evaluated by raising the voltage up to the maximum test voltage, U_{test}, which is derived from the peak voltage at the motor terminals, U_p. The voltage U_p depends on the dc bus voltage, U_{dc}, through the overshoot factor, OF.

$$U_p = U_{\mathrm{dc}} \cdot \mathrm{OF}. \tag{1}$$

The value of OF depends on the cable length and on the rise time of the voltage surge at the converter terminals. For the SyrNemo machine, since the inverter is directly connected to the motor, the OF would be 1. Indeed, we decided to test with OF $= 1.5$ to provide a more conservative evaluation.

The test levels are determined according to the following equation [18]:

$$U_{\mathrm{test}} = U_p \cdot K \cdot \mathrm{EF} \tag{2}$$

where K is the insulation system factor [18], i.e., a factor that models (based on empirical evidence and worst case criteria) the propagation of the peak voltage across the insulation subsystems. In particular:

1) phase/phase insulation subsystem: $K = 1$;
2) phase/ground insulation subsystem: $K = 0.7$;
3) turn/turn insulation subsystem: $K = 0.7$.

EF is the Enhancement Factor. The EF value was decided by the IEC Technical Committee based on empirical considerations. The standard provides EF value ranges, which depend on the insulation subsystem. Fort the SyrNemo motor, the highest values for each insulation subsystem were selected, and are as follows:

1) phase/phase insulation subsystem: EF $= 1.63$;
2) phase/ground insulation subsystem: EF $= 1.38$;
3) turn/turn insulation subsystem: EF $= 1.63$.

The test levels obtained through the standard procedure and reported in Table II are suitable for qualification purposes.

It is worthwhile to note that electrical stress of the turn insulation does not take into account the fact that, in a hairpin machine, the turn voltage is generally well below the voltage estimated through (2) (which provides a conservative estimate for random-wound systems, where the first and last turn in a coil might be physically adjacent). Thus, for the qualification tests performed here, the electrical stress has been purposely raised to provide a more conservative qualification procedure.

C. Test Bench

A forced air convection oven was employed. The oven has a 60-mm hole on the lateral surface to permit the transmission of mechanical vibration in the sample inside the oven. The mechanical stress has been generated by a 2110E shaker system supplied by Modal Shop. The vibration profile employed followed the one previously showed in Fig. 2 and its input signal has been supplied by a waveform generator through a user-defined waveform. An accelerometer has been used to record the vibration on the samples, at the beginning of each aging process, ensuring that the power spectral density of the acceleration on the samples was matching that described [21]. Fig. 4 shows pictures of the main part of the test bench.

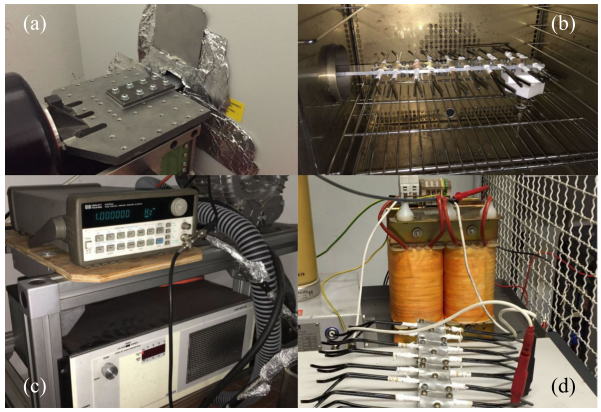

Fig. 4. Test bench particulars: (A) shaker; (B) samples and sample holder inside the oven; (C) waveform generator and shaker amplifier; and (D) samples during PD tests.

Since the sample was inside the oven while the vibrating bench was outside, connected through a metal bar, the weight of the sample would apply a too large torque to the vibrating bench in the absence of any support. Therefore, a proper support system capable of sustaining the samples without influencing the mechanical stress and without transmitting it to the oven was devised. Due to the different shape and weight of formettes and coupled bars, two different systems were designed. For the formettes, a steel spring support was devised. The rod with the multiple coupled bars has simply laid on a PTFE cylinder.

After cooling down the samples, PDIV levels were investigated. The test system adopted is a classical PD detection circuit [22], [23]. The samples have been connected to the HV supplied by a voltage transformer connected to a pacific source voltage generator and a to a 1-nF capacitance in parallel. The PD signals have been recorded through a PDBase supplied by Techimp.

Eventually, the samples were set inside a climatic chamber with saturated air at room temperature for 1 h.

IV. EXPERIMENTAL RESULTS

A. Phase-to-Ground Insulation

Before starting the aging procedure, the phase-to-phase and phase-to-ground insulation of each formette were tested at 700 $\mathrm{V_{rms}}$ for few minutes. No PDs were detected, meaning that the design was correct and the insulation was free of manufacturing defect.

The first formette was aged at 250 °C with the procedure explained in Section III-B. During 15 aging subcycles, all conductors were still able to withstand the applied voltage and PD activity could not be detected. Since the average lifetime of the samples should be ten cycles, the test was stopped to inspect the formette. A visual examination highlighted a large number of

Fig. 5. End winding of the formette after 15 aging subcycles at 250 °C.

insulating film fractures and the total detachment of the enamel from the copper bars in some spots as shown in Fig. 5. Thus, the dielectric withstand capability of the turn-to-turn insulation was investigated by applying voltage between adjacent conductors. Most of the bars had an immediate breakdown at 200–250 V without any PD.

Therefore, it was possible to conclude that, in the absence of PD, the slot liners are extremely more resistant to temperature and mechanical stress than the enamel. As a consequence, the phase-to-ground and phase-to-phase insulation systems reliability and lifetime are well in excess of those of the turn-to-turn insulation system. Therefore, further investigations on formettes were interrupted.

B. Turn-to-Turn Insulation

The coupled bars used as a model for the turn-to-turn insulation were placed on an aluminum rod as shown in Fig. 1. Also in this case, no PD were recorded during preliminary tests, ensuring that the insulation was in perfect condition even in the absence of impregnation (worst case condition for the insulation) before starting the aging process.

The simultaneous thermal and mechanical tests, as described in the previous chapters, were carried out at three different temperatures: 250 °C, 240 °C, and 220 °C in order to obtain a trustworthy regression curve. Unexpectedly, the bars did not suffer PD at all. Breakdown occurred while ramping up the voltage for PD testing, in the absence of PD.

Data were collected and examined by the Weibull probability distribution

$$F(t) = 1 - e^{-(t/\alpha)^{\beta}} \tag{3}$$

where F is the cumulative distribution function of the lifetime, t is the lifetime, α is the scale parameter (63.2% percentile of lifetime), and β is the shape parameter (the larger the β, the lower is the variance of the lifetime). In order to estimate α and β in (3), the dataset must be ordered in ascending order and the Weibull distribution linearized

$$\ln(-\ln(1 - F(t_i))) = \beta \ln(t_i) - \beta \ln(\alpha) \tag{4}$$

where t_i is one of the experimental outcomes (in total $n = 10$ for the datasets described here) Then, $F(t_i)$ is estimated using

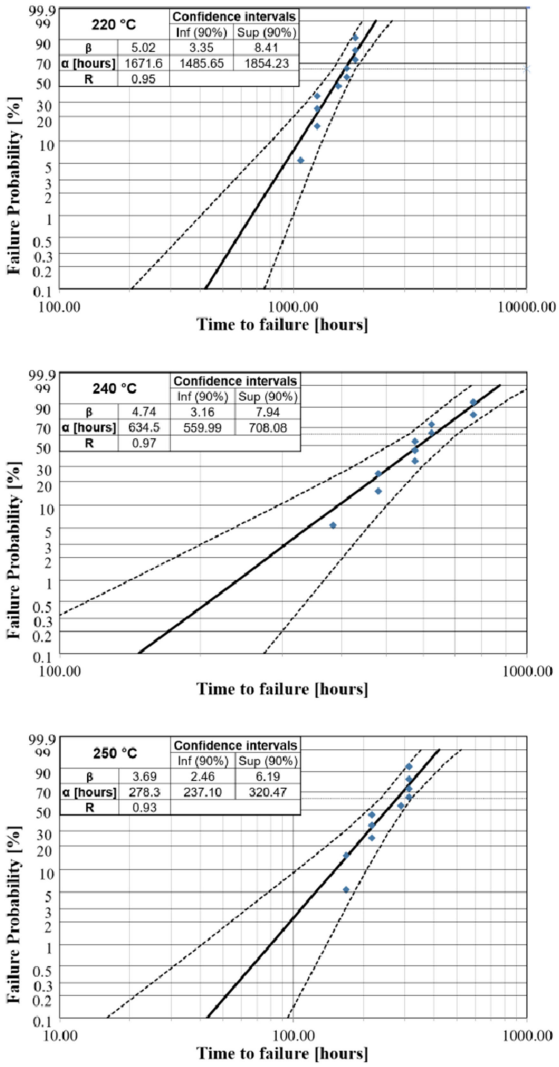

Fig. 6. Weibull cumulative probability distribution and parameters for (top) 220 °C; (center) 240 °C; (bottom) 250 °C.

the median rank estimator as

$$\hat{F}(t_i) = \frac{i - 0.3}{n + 0.4}. \tag{5}$$

The scale and shape parameter distribution of the Weibull distribution for the lifetime of the coupled bars can thus be derived using linear regression applied to (4). The results of this procedure applied to each dataset are reported in Fig. 6.

The samples were visually investigated during the aging process, except in the region where the conductors were in intimate contact, avoiding to change their mutual position. In several points, cracks and rupture lines were detected. An example is shown in Fig. 7. Clearly, these damages bring the insulation to breakdown when appearing on the bar surfaces that are in mutual contact, the final breakdown mechanism being excessive leakage current with local melting of the insulation.

A further investigation was carried out on the coupled bars. New samples were aged following the same procedure described before, but without any mechanical stress. The aging temperature was 240 °C, in order to compare this result with the ones obtained before at the same temperature with the vibrations. The re-

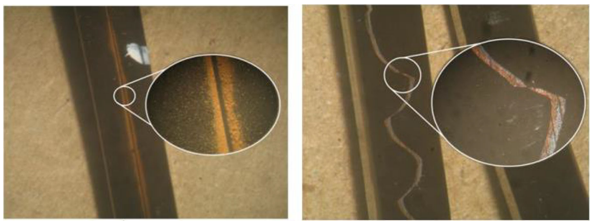

Fig. 7. Optical microscope imaging of insulation after thermomechanical aging.

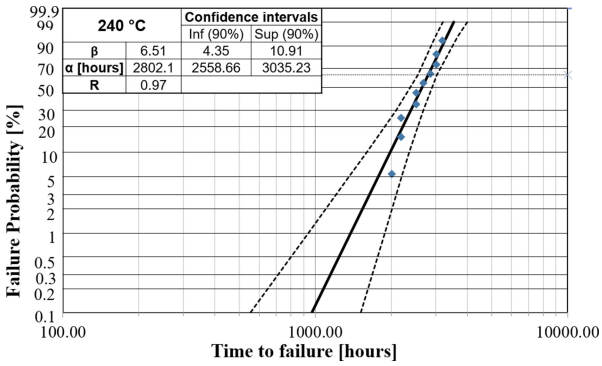

Fig. 8. Weibull cumulative probability distribution and parameters for samples tested at 240 °C without mechanical stress.

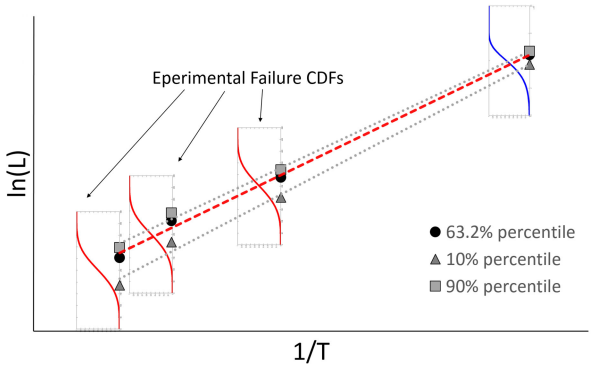

Fig. 9. Sketch representation of the procedure used to extrapolate the failure time distribution at 180 °C.

sults are presented in Fig. 8. The sample lifetime is significantly longer than in Fig. 6 (the chart in the middle) when the specimens were subjected to both temperature and mechanical stress.

V. Lifetime Extrapolation

The aim of qualification tests is to obtain a reliable value of a component lifetime under given operating conditions [24]. For the SyrNemo insulation, 180 °C was chosen as the operating temperature, taking into account a safety margin on the hot-spot temperature estimated from thermal simulation models resorting to typical driving cycles.

A common assumption in lifetime tests performed at different temperatures is to consider valid the Arrhenius equation that models the reaction rate, R, of the chemical reaction that promotes fastest degradation as

$$R \;=\; \Pi \cdot e^{-E_a/k_B T} \tag{6}$$

where Π is the preexponential constant, E_a is the activation energy (of the chemical reaction), k_B is the Boltzmann constant, and T is the temperature in Kelvin. It is worthwhile to observe that, for an insulation systems subjected to multiple stresses, Π and E_a are functions of the employed materials and of the other stresses applied to the insulation (e.g., mechanical vibrations and electrical stress). However, since the tests discussed here were carried out keeping all other stresses at a constant level, this dependence will not be highlighted in the following.

Assuming a constant reaction rate, the lifetime L is the time required to achieve a critical aging level, A_C, bringing the insulation to failure

$$L \cdot R \;=\; L \cdot \Pi \cdot e^{-E_a/RT} \;=\; A_C . \tag{7}$$

Considering now a generic temperature T and a reference temperature T_0 (corresponding to a reference lifetime L_0) as

$$L_T \cdot \Pi \cdot e^{-E_a/RT} \;=\; L_0 \cdot \Pi \cdot e^{-E_a/RT_0} \tag{8}$$

$$\ln L_T \;=\; \ln L_0 - \frac{E_a}{R}\left(\frac{1}{T} - \frac{1}{T_0}\right). \tag{9}$$

Thus, by taking $C = \ln L_0 + E_a/(RT_0)$ and $B = E_a/R$, it is it possible to obtain

$$\ln\,(L) \;=\; C + B\frac{1}{T} \tag{10}$$

that is, $\ln\,(L)$ is a linear function of $1/\mathrm{T}$. Thus, the results at the three different temperatures should align on a $\ln\,(L)$ versus $1/\mathrm{T}$ plot, and the life model parameters B and C can be determined through linear regression. Eventually, by inserting the estimated B and C values in (10), extrapolation of the results of the sample lifetime at 180 °C becomes possible.

Indeed, the lifetime is a random variable, thus L must be a statistic of the experimental failure times, and (10) can be applied to different statistics as, e.g., the mean value, the median or other percentiles of the sample distribution of failure times. In order to assess the reliability of the insulation considered here, we decided to use the percentiles obtained by fitting the experimental data by the Weibull distribution. Extrapolation was carried out for 16 different percentiles (from 0.1% up to 99.9% probability). The procedure used is sketched in Fig. 9. It is interesting to observe that the minimum correlation coefficient obtained in the extrapolation procedure is 0.968 (associated with the 0.1% percentile). This confirms that the Arrhenius law is an effective approximation of the phenomenon within the range of temperatures used for the tests.

Eventually, a Weibull probability distribution has been fitted to the extrapolated percentiles. The procedure is based on (4), but t_i is one of the percentiles obtained by extrapolation, and $F(t_i)$ is the probability of the percentile itself. The extrapolated percentiles and their associated probability values are reported in Fig. 10. Following this procedure, the scale and shape parameter distribution of the Weibull distribution for the lifetime of the coupled bars at 180 °C were evaluated as $\alpha = 25\ 436$ h and $\beta = 10.59$.

Since the electrical motor winding consists of a number of hairpin bars in contact between them, it can be regarded as a reliability system with N identical items in series. Owing to

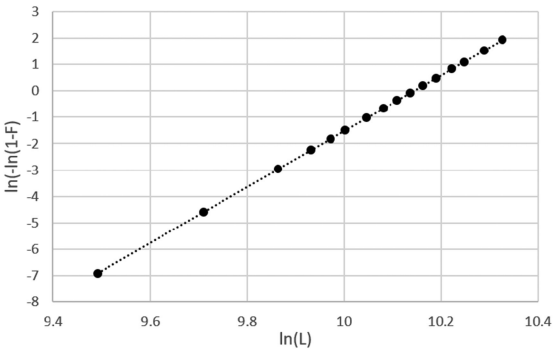

Fig. 10. Weibull chart reporting the percentiles of the failure time distribution extrapolated at a temperature of 180 °C.

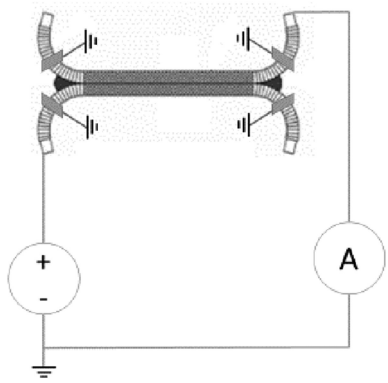

Fig. 11. Test setup for polarization current measurements in a turn-to-turn sample.

the properties of the Weibull distribution, the distribution of the system can be determined from that of the items by scaling the α of the items by $1/N^{1/\beta}$ to determine the Weibull scale parameter of the system α_s. Considering the feature of the SyrNemo motor winding (4 bars per slot, thus 3 failure modes per slot, 24 slots per phase), $N = 72$. Thus

$$\alpha_s = \frac{\alpha}{N^{\frac{1}{\beta}}} = \frac{25\,436 \text{ h}}{72^{\frac{1}{10.59}}} = 16\,985 \text{ h}. \quad (11)$$

At $L = 10\,000$ h, the target lifetime of the motor, the insulation reliability, R_s can be estimated as

$$R_s\ (10\,000) = e^{-(10\,000/16{,}985)^{\beta}} = 99.6\% \quad (12)$$

which seems fairly acceptable also considering that a number of conservative assumptions were made to design the qualification tests.

VI. Diagnostics by Polarization Current Measurements

The possibility to analyze the degradation of the turn-to-turn insulation has been evaluated through the polarization current measurement. The study focuses on the analysis of the polarization current trend for every single sample, comparing the outputs on an aging subcycle per subcycle basis.

The test was carried out applying a dc voltage at the terminals of a pair of coupled bars as shown in Fig. 11. The turn-to-turn coupling was connected to the dc voltage supply (High Voltage Supply 248—Keithley) on one extremity, while the other end was connected to the electrometer (System Electrometer 6514—Keithley) that indicates the polarization current reading. Each measurement on a single sample lasted 10 min. In order to minimize the surface current contribution, a guard ring, connected to the ground, was placed on each bar extremity.

The tests have been carried out on the bars aged at 220 °C. The trend of each sample has been recorded at the end of every aging subcycle, after the PD measurement. Fig. 12 shows the measurements obtained for one representative sample in three different subcycles, until breakdown. The polarization current is about constant during the aging subcycles, except a significant increase can be observed at the end of the subcycle that preceded breakdown.

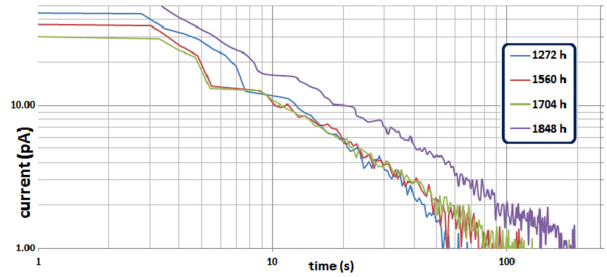

Fig. 12. Polarization current measurements in function of the aging time.

These results are, at their present stage, more qualitative than quantitative. However, it is interesting to observe that polarization current (or insulation resistance) measurements, the simplest diagnostic test in the toolbox, can be of use to diagnose an excessive wear of the insulation system in inverter-fed motors, where PDs are the predominant concern. The obvious caveat is that PD should not be incepted during operation.

VII. Discussion

One of the key factors that may bring the reliability of the inverter-fed motor to unacceptable levels is the inception of PD. To prevent PD inception in an insulation system, the insulation should have an adequate thickness [25]. Tests performed on twisted pairs confirm that the PDIV scale almost linearly with the conductor insulation thickness, see, e.g., Fig. 13. The findings reported in this paper demonstrate that, if the conductor insulation is thick enough to ensure that PD do not take place at all times during the aging tests, breakdown will occur due to the combined action of mechanical and thermal stresses. This will induce cracks and abrasions in the insulation, where the leakage current could become large enough to melt the insulation.

Following [20], the best procedure to carry out aging subcycles would be applying thermal and mechanical stresses simultaneously. Unfortunately, within the time frame of the project, we had no time to verify systematically this point (i.e., by performing aging tests where thermal and mechanical stress are applied in sequence rather than simultaneously during aging subcycles). However, the results of tests with temperature only

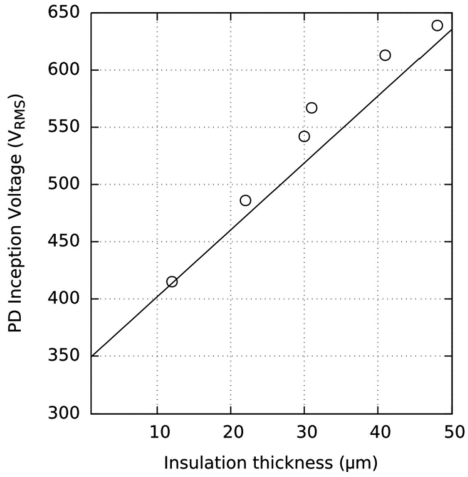

Fig. 13. PDIV as a function of insulation thickness in twisted pairs (taken from [25]).

and the visual observation that the dielectric is removed by the combined action of the two stress during multifactorial tests seems to confirm this point.

In the absence of PD, the turn-to-turn insulation is the weakest part of the whole motor, and consequently, is the one determining its lifetime. As a matter of fact, the resistance to thermomechanical aging of the aramidic paper ensures high performance to the phase-to-phase and phase-to-ground insulation subsystems. Indeed, since aramidic papers are not able to withstand well PD, if the risk of PD inception is nonnegligible, this point should not be considered.

The IEC 60034-18-41 standard should be improved by considering that some stator windings are PD free by manufacturing, other by design. To the first class belong motors with an insulation thickness that is not large enough to ensure that PD will not occur during operation. These motors require impregnation to fill in the air pockets adjacent to the conductors, thus, preventing PD inception. After a sufficiently long exposure time to thermal and mechanical stresses, impregnation depolymerizes becoming brittle and it is removed from the insulation. In a motor supplied by ac sinusoidal waveforms (50/60 Hz), this will be a step toward breakdown, but the residual life could still be large enough to ensure sufficient reliability. On the contrary, in an inverter-fed motor, this will give rise to partial discharge inception, and consequently, to premature breakdown. Therefore, it is of greater importance to carry out qualification using PD inception as an endpoint. However, for a motor whose insulation is large enough to prevent PD (i.e., PD free by design), impregnation could be a way to improve thermal exchange and mechanical tightness of the conductors, but breakdown will not occur by PD-induced degradation, and the use of IEC 60034-18-41 qualification is debatable.

Also, if an insulation system is PD free by design, the breakdown mechanisms (cracks giving rise to excessive leakage currents) does not depart from that typical of motors fed by ac 50/60-Hz sinusoidal voltages. For this type of motors, the "reference system" could be the insulation system itself, if it has proved to behave satisfactorily under sinusoidal waveforms.

VIII. Conclusion

This paper provides information that could be of use to improve the IEC 60034-18-41 standard or other would-be standards related more specifically to EV insulation qualification (to our best knowledge, nothing specific exists to date within the body of IEC and IEEE standards). The concept that inverter-fed machines can be separated in machines that are PD free by design and machines that are liable to become site of PD activity after a sufficiently long exposure time could help to develop a more rational approach to the issue of inverter-fed machine qualification, possibly reducing the costs for the end user.

References

[1] M. Weiss *et al.*, "Will euro 6 reduce the NO_x emissions of new diesel cars? Insights from on-road tests with portable emissions measurement systems (PEMS)," *Atmos. Environ.*, vol. 62, no. 2, pp. 657–665, 2012.

[2] 2015. [Online]. Available: www.afdc.energy.gov

[3] J. Gragger *et al.*, "Design features of an innovative synchronous reluctance machine for battery electric vehicles applications," SAE Tech. Paper 2016-01-1235, 2016.

[4] J. Juergens, O. Winter, and A. Fricassé, "Influences of iron loss coefficients estimation on the prediction of iron losses for variable speed motors," in *Proc. IEEE Int. Elect. Mach. Drives Conf.*, 2015, pp. 1254–1259.

[5] M. Hernandez *et al.*, "Environmental impact of traction electric motors for electric vehicles applications," *Int. J. Life Cycle Assessment*, pp. 1–12, 2015.

[6] E. Schlemmer and H. Lausegger-Rauch, "E-drive component tests derived from vehicle master test cases in the syrnemo collaborative research project," in *Proc. Int. Conf. Renewable Energies Power Quality*, 2016, no. 14, pp. 166–171.

[7] H. A. Toliyat and G. B. Kliman, *Handbook of Electrical Motor*. Boca Raton, FL, USA: CRC Press, 2004.

[8] T. Shugg, *Handbook of Electrical and Electronic Insulation Materials*, 2nd ed. Piscataway, NJ, USA: IEEE Press, 1995.

[9] G. C. Stone, E. A. Boulter, I. Culbert, and H. Dhirani, *Electrical Insulation for Rotating Machines—Design, Evaluation, Aging, Testing, and Repair*, Piscataway, NJ, USA: IEEE Press, 2004.

[10] J. H. Dymond *et al.*, "Stator winding failures: Contamination, surface discharge, tracking," *IEEE Trans. Ind. Appl.*, vol. 38, no. 2, pp. 577–583, Mar./Apr. 2002.

[11] J. C. G. Wheeler, "Environmental factors affecting mechanical performance of composites in service," in *Proc. IEE Colloq. Mech. Influence Elect. Insul. Perform.*, 1995, pp. 6–9.

[12] H. Hirose, "A method to estimate the lifetime of solid electrical insulation," *IEEE Trans. Elect. Insul.*, vol. EI-22, no. 6, pp. 745–753, Dec. 1987.

[13] M. Kaufhold, H. Auinger, M. Berth, J. Speck, and M. Eberhardt, "Electrical stress and failure mechanism of the winding insulation in PWM-inverter-fed low-voltage induction motors," *IEEE Trans. Ind. Electron.*, vol. 47, no. 2, pp. 396–402, Apr. 2000.

[14] *High-Voltage Test Techniques—Partial Discharge Measurements*, IEC 60270, 2000.

[15] R. J. Kerkman, S. Member, D. Leggate, and G. L. Skibinski, "Interaction of drive modulation and cable parameters on AC motor transients," *IEEE Trans. Ind. Appl.*, vol. 33, no. 3, pp. 722–731, May/Jun. 1997.

[16] A. Cavallini, D. Fabiani, and G. C. Montanari, "Power electronics and electrical insulation systems—Part 1: Phenomenology overview," *IEEE Elect. Insul. Mag.*, vol. 26, no. 3, pp. 7–15, May/Jun. 2010.

[17] A. Cavallini, D. Fabiani, and G. C. Montanari, "Power electronics and electrical insulation systems—Part 2: Life modeling for insulation design," *IEEE Elect. Insul. Mag.*, vol. 26, no. 4, pp. 33–39, Jul./Aug. 2010.

[18] Partial Discharge Free Electrical Insulation Systems (Type I) Used in Rotating Electrical Machines Fed From Voltage Converters—Qualification and Quality Control Tests, IEC 60034-18-41, 2014.

[19] *Functional* Evaluation *of* Insulation Systems—*Test* Procedures *for* Wire-Wound Windings—*Thermal* Evaluation *and* Classification, IEC 60034-18-21, 2012.

[20] Evaluation and Qualification of Electrical Insulation Systems, IEC 60505, 2011.

[21] *Road Vehicles—Environmental Conditions and Testing for Electrical and Electronic Equipment—Part 3: Mechanical Loads*, ISO 16750-3, 2012.

[22] A. Cavallini, D. Fabiani, and G. C. Montanari, "Power electronics and electrical insulation systems–Part 3: Diagnostic properties," *IEEE Elect. Insul. Mag.*, vol. 26, no. 5, pp. 30–40, Sep./Oct. 2010.
[23] G. C. Stone, "Partial discharge diagnostics and electrical equipment insulation condition assessment," *IEEE Trans. Dielect. Elect. Insul.*, vol. 12, no. 5, pp. 891–903, Oct. 2005.
[24] L. A. Escobar and W. Q. Meeker, "A review of accelerated test models," *Stat. Sci.*, vol. 21, no. 4, pp. 552–577, 2006.
[25] L. Lusuardi *et al.*, "Design criteria for inverter-fed type 1 motors," in *Proc. Int. Conf. Dielect.*, 2016, pp. 605–608, doi: 10.1109/ICD.2016.7547528.

Paolo Mancinelli was born on December 1988. He received the B.Eng. and M.Eng. degrees in energy engineering from the University of Bologna, Bologna, Italy, in 2010 and 2013, respectively. He is currently working toward the Ph.D. degree in electrical engineering at the Department of Electrical Electronics and Information Engineering, University of Bologna and the Engineering Department, University of Leicester, Leicester, U.K.

His main research interests include nanodielectric, field grading material, electrical treeing inside both solids and gels, aging investigation, qualification and diagnosis of power system insulation, and motor windings subjected to fast repetitive pulses.

Simone Stagnitta was born in Catania, Italy, in 1988. He received the B.E. degree in mechanical engineering from the University of Catania, Catania, Italy, in 2012, and the M.Eng. degree in energy engineering from the University of Bologna, Bologna, Italy, in 2016.

In 2011, he worked on the project "Programma Operativo Interregionale Energie Rinnovabili e Risparmio Energetico," approved by the European Commission, about the energy requalification of San Giovanni La Punta School Complex. In 2015, he joined the Laboratory of Innovation Technologies, University of Bologna, taking part in the European Project "SyrNemo."

Andrea Cavallini was born in December 1963. He received the M.Eng. and Ph.D. degrees from the University of Bologna, Bologna, Italy, in 1990 and 1995, respectively.

He is currently working at the University of Bologna. His research interests include the effect of nonsinusoidal waveforms on partial discharge activity and degradation of different insulation systems, modeling of partial discharge inception voltages using streamer inception criteria for design purposes, the dielectric withstand properties of insulating fluids as natural and synthetic esters and nanofluids, diagnostics of insulation systems. He is an Adcom member of the IEEE Dielectric and Electric Insulation Society and is currently the Chair of the Education committee of the same society.